THE ASTROPHYSICAL JOURNAL, 497:178–187, 1998 April 10

MULTIWAVELENGTH OBSERVATIONS OF A DRAMATIC HIGH-ENERGY FLARE IN THE BLAZAR 3C 279

A. E. WEHRLE,[1] E. PIAN,[2,3] C. M. URRY,[2] L. MARASCHI,[4] I. M. MCHARDY,[5] A. J. LAWSON,[5] G. GHISELLINI,[6] R. C. HARTMAN,[7] G. M. MADEJSKI,[7] F. MAKINO,[8] A. P. MARSCHER,[9] S. J. WAGNER,[10] J. R. WEBB,[11,12] G. S. ALDERING,[13] M. F. ALLER,[14] H. D. ALLER,[14] D. E. BACKMAN,[15] T. J. BALONEK,[16] P. BOLTWOOD,[17] J. BONNELL,[7] J. CAPLINGER,[7] A. CELOTTI,[18] W. COLLMAR,[19] J. DALTON,[15] A. DRUCKER,[15] R. FALOMO,[20] C. E. FICHTEL,[7] W. FREUDLING,[21] W. K. GEAR,[22] N. GONZALEZ-PEREZ,[23] P. HALL,[24] H. INOUE,[8] W. N. JOHNSON,[25] D. KAZANAS,[7] M. R. KIDGER,[23] T. KII,[8] R. I. KOLLGAARD,[26] Y. KONDO,[7] J. KURFESS,[25] Y. C. LIN,[27] B. MCCOLLUM,[7] K. MCNARON-BROWN,[25] F. NAGASE,[8] A. D. NAIR,[28] S. PENTON,[29] J. E. PESCE,[2,30] M. POHL,[19] C. M. RAITERI,[31] M. RENDA,[15] E. I. ROBSON,[22,32] R. M. SAMBRUNA,[7,30] A. F. SCHIRMER,[16] C. SHRADER,[7] M. SIKORA,[33] A. SILLANPÄÄ,[34] P. S. SMITH,[35] J. A. STEVENS,[32] J. STOCKE,[29] L. O. TAKALO,[34] H. TERÄSRANTA,[36] D. J. THOMPSON,[7] R. THOMPSON,[7] M. TORNIKOSKI,[36] G. TOSTI,[37] A. TREVES,[38] P. TURCOTTE,[15] S. C. UNWIN,[39] E. VALTAOJA,[36] M. VILLATA,[31] W. XU,[1] A. YAMASHITA,[8] AND A. ZOOK[40]

Received 1997 July 25; accepted 1997 November 18

ABSTRACT

The blazar 3C 279, one of the brightest identified extragalactic objects in the γ-ray sky, underwent a large (factor of ~ 10 in amplitude) flare in γ-rays toward the end of a 3 week pointing by *Compton Gamma Ray Observatory* (*CGRO*), in 1996 January–February. The flare peak represents the highest γ-ray intensity ever recorded for this object. During the high state, extremely rapid γ-ray variability was seen, including an increase of a factor of 2.6 in ~ 8 hr, which strengthens the case for relativistic beaming. Coordinated multifrequency observations were carried out with *Rossi X-Ray Timing Explorer* (*RXTE*), *Advanced Satellite for Cosmology and Astrophysics* (*ASCA; or*, *Astro-D*), *Roentgen Satellite* (*ROSAT*), and *International Ultraviolet Explorer* (*IUE*) and from many ground-based observatories, covering most accessible wavelengths. The well-sampled, simultaneous *RXTE* light curve shows an outburst of lower amplitude (factor of $\simeq 3$) well correlated with the γ-ray flare without any lag larger than the temporal resolution of ~ 1 day. The optical-UV light curves, which are not well sampled during the high-energy flare, exhibit more modest variations (factor of ~ 2) and a lower degree of correlation. The flux at millimetric wavelengths was near a historical maximum during the γ-ray flare peak, and there is a suggestion of a correlated decay. We present simultaneous spectral energy distributions of 3C 279 prior to and near to the flare peak. The γ-rays vary by more than the square of the observed IR–optical flux change, which poses some problems for specific blazar emission models. The synchrotron self-Compton (SSC) model would require that the largest synchrotron variability occurred in the mostly unobserved submillimeter/far-infrared region. Alternatively, a large variation in the external photon field could occur over a timescale of a few days. This occurs naturally in the "mirror" model, wherein the flaring region in the jet photoionizes nearby broad emission line clouds, which, in turn, provide soft external photons that are Comptonized to γ-ray energies.

Subject headings: galaxies: photometry — gamma rays: observations — quasars: individual (3C 279) — radiation mechanisms: nonthermal

[1] Infrared Processing Analysis Center, MC 100-22, Jet Propulsion Laboratory and California Institute of Technology, Pasadena, CA 91125.
[2] Space Telescope Science Institute, 3700 San Martin Drive, Baltimore, MD 21218.
[3] ITESRE-CNR, Via Gobetti 101, I-40129 Bologna, Italy.
[4] Osservatorio Astronomico di Brera, Via Brera 28, I-20121 Milan, Italy.
[5] Department of Physics, University of Southampton, Southampton SO9 5NH, England, UK.
[6] Osservatorio Astronomico di Brera, Via Bianchi 46, I-22055 Merate (Lecco), Italy.
[7] NASA/Goddard Space Flight Center, Greenbelt, MD 20771.
[8] ISAS, 3-1-1, Yoshinodai, Sagamihara, Kanagawa 229, Japan.
[9] Department of Astronomy, Boston University, 725 Commonwealth Avenue, Boston, MA 02215.
[10] Landessternwarte, Heidelberg-Königsstuhl, D-69117 Heidelberg, Germany.
[11] Department of Physics, Florida International University, University Park, Miami, FL 33199.
[12] SARA Observatory, KPNO/NOAO, 950 North Cherry Avenue, P.O. Box 26732, Tucson, AZ 85726.
[13] University of Minnesota, Department of Astronomy, 116 Church Street, SE Minneapolis, MN 55455.
[14] University of Michigan, Physics and Astronomy, 817 Dennison Building, Ann Arbor, MI 48109.
[15] Franklin & Marshall College, Physics and Astronomy Department, P.O. Box 3003, Lancaster, PA 17604-3003.
[16] Colgate University, Department of Physics and Astronomy, 13 Oak Drive, Hamilton, NY 13346-1398.
[17] 1655 Main Street, Stittsville, Ontario, Canada K2S 1N6.
[18] SISSA/ISAS, Via Beirut 2-4, I-34014 Miramare-Grignano (Trieste), Italy.
[19] Max Planck-Institut für Extraterrestrische Physik, Giessenbachstrasse, D-85740 Garching, Germany.
[20] Osservatorio Astronomico di Padova, Via Osservatorio 5, I-35122 Padova, Italy.
[21] Space Telescope European Coordinating Facility, Karl-Schwarzschild Strasse 2, D-85748 Garching, Germany.

1. INTRODUCTION

The remarkable emission of blazars in the MeV–GeV energy range, relativistically enhanced by Doppler beaming, has made them the only class of active galactic nuclei detected by the EGRET instrument on *Compton Gamma Ray Observatory* (*CGRO*) (Thompson et al. 1995). The quasar 3C 279 ($z = 0.538$), the first radio source in which superluminal motion was discovered, is a prototype of the blazar class. It is the second brightest γ-ray blazar (Kniffen et al. 1993), the brightest being PKS 1622−297 (Mattox et al. 1997). Violent variability is a distinguishing property of blazars, and the γ-ray emission is no exception, varying with large amplitude on timescales of days or less (see recent review by Hartman 1996), implying a very compact emission region.

The radio-to-UV continuum from blazars is commonly interpreted as synchrotron radiation from high-energy electrons in a relativistic jet, while the MeV–GeV photons are believed to be emitted via inverse Compton scattering of soft seed photons by the same electrons (e.g., Ulrich, Maraschi, & Urry 1997). Finding correlations among the variations at high (X- to γ-ray) and low frequencies is, therefore, critical to understanding which ranges of the Compton and synchrotron components result from the same electrons and to clarifying the nature of the seed photons available for scattering: namely, whether they are generated within the jet (synchrotron self-Compton, or SSC) or in regions external to the jet, like the accretion disk or the broad emission line clouds (external Compton, or EC).

Multiwavelength observations of blazars in conjunction with EGRET pointings have been obtained at several epochs. However, either the monitoring was too sparse or the source was not active during the campaign, so detections of correlated, multiwavelength variability on short timescales are tentative (3C 279, Maraschi et al. 1994; Hartman et al. 1996; OJ 287, Webb et al. 1996; PKS 0537−441, Pian et al. 1998).

A comparison of the spectral energy distribution of 3C 279 during the historically brightest state of the source (1991 June) with the lowest state ever observed (1992 December–1993 January) showed that the γ-ray flux variation between the two epochs was larger than at any other wavelength (Maraschi et al. 1994), as predicted qualitatively by the SSC model (Maraschi, Ghisellini, & Celotti 1992). Multiwavelength variability between 1991 June and October was found to follow the same behavior (Hartman et al. 1996). The larger γ-ray variability could also be accommodated within an EC scenario, provided there was a change in the bulk Lorentz factor of the γ-ray–emitting plasma or the external photon field varied for some other reason, possibly as a result of enhanced photoionization of surrounding broad emission line clouds by the jet itself.

The multiwavelength campaign on 3C 279 in 1996 January–February was organized as a 2 week coordinated program of the *CGRO*, the *Roentgen Satellite* (*ROSAT*), the *Rossi X-Ray Timing Explorer* (*RXTE*), and the *IUE* spacecraft, plus a 1 week Target of Opportunity extension triggered by the high intensity measured with EGRET during the first week. The aim was to follow the evolution of a short-timescale outburst at all frequencies in order to constrain the possibility of a variation of the bulk Lorentz factor. This would allow discrimination between the possible models and clarification of the nature of the seed photons being inverse Compton scattered to γ-ray energies.

The campaign also benefited from the simultaneous and quasi-simultaneous observations with the *Hubble Space Telescope* (*HST*), the *Advanced Satellite for Cosmology and Astrophysics* (*ASCA; or, Astro-D*), and the *Infrared Space Observatory* (*ISO*), as well as with many ground-based radio and optical telescopes. The final data set is rich in both temporal and wavelength coverage to an extent unmatched by any other blazar.

In this paper we present the observations conducted at the radio to γ-ray facilities participating in the multiwavelength monitoring (§ 2), the light curves obtained (§ 3), and the spectral energy distributions before and near the flare peak (§ 4). We then compare our results with those at previous epochs, discuss constraints on theoretical models (§ 5), and summarize our findings (§ 6).

2. OBSERVATIONS

In the following we give the essential information on the observations at each wavelength and summarize the results in Table 1. The multiwavelength light curves of 3C 279 from 1996 January 11 through 1996 February 13 are shown in Figure 1 on a logarithmic scale. Included are data with the most complete temporal coverage and at the full range of wavelengths. We defer to separate papers for a complete presentation and for details about data analysis. In particular, a complete account of the γ-ray, X-ray, and *ISO* observations, data reduction, and analysis will be given in Hartman et al. (1998), McHardy et al. (1998), and Barr et al. (1998), respectively.

[22] Centre for Astrophysics, University of Central Lancashire, Preston, PR1 2HE, England, UK.
[23] Instituto de Astrofísica de Canarias, E-38200, La Laguna, Tenerife, Spain.
[24] Steward Observatory, University of Arizona, Tucson, AZ 85721.
[25] Naval Research Laboratory, 4555 Overlook Avenue, SW Washington, DC 20375-5352.
[26] Fermi National Accelerator Laboratory, Kirk Road and Pine Street, Batavia, IL 60510.
[27] W. W. Hansen Experimental Physics Laboratory and Department of Physics, Stanford University, Stanford, CA 94305.
[28] Department of Astronomy, University of Florida, Gainesville, FL 32601.
[29] University of Colorado, JILA, Campus Box 440, Boulder, CO 80309-0440.
[30] Pennsylvania State University, Deptartment of Astronomy, 525 Davey Lab, University Park, PA 16802.
[31] Osservatorio Astronomico di Torino, Strada Osservatorio 20, I-10025 Pino Torinese, Italy.
[32] Joint Astronomy Centre, 660 North Aohoku Place, University Park, Hilo, HI 96720.
[33] Copernicus Astronomical Center, Polish Academy of Science, Warsaw, Poland.
[34] Tuorla Observatory, Tuorla 21500 Piikkiö, Finland.
[35] NOAO/KPNO, North Cherry Avenue, P.O. Box 26732, Tucson, AZ 85726.
[36] Metsähovi Radio Research Station, 02540 Kylmala, Finland.
[37] Osservatorio Astronomico, Università di Perugia, I-06100 Perugia, Italy.
[38] Department of Physics, University of Milan at Como, Via Lucini 3, I-22100 Como, Italy.
[39] MS 306-388, Jet Propulsion Laboratory, California Institute of Technology, 4800 Oak Grove Drive, Pasadena, CA 91109.
[40] Pomona College, Department of Physics and Astronomy, 610 College Avenue, Claremont, CA 91711-6359.

TABLE 1

JOURNAL OF 1996 MULTIWAVELENGTH OBSERVATIONS OF 3C 279

Instrument	Band	Observer (PI)	log ν (Hz)	Dates (January)	log $\langle f_{\rm min}\rangle$[a] (ergs s^{-1} cm^{-2} Hz^{-1})	Dates (February)	log $\langle f_{\rm max}\rangle$[a] (ergs s^{-1} cm^{-2} Hz^{-1})
CGRO/EGRET	30–10000 MeV	Hartman & Wehrle	22.98	25–28	$-32.54^{+0.15}_{-0.23}$ (4)	4.1–5.7	$-31.80^{+0.12}_{-0.16}$ (6)
CGRO/Comptel	10–30 MeV	Collmar	21.68	16–30	$-31.15^{+0.19}_{-0.34}$	1–6	$-30.60^{+0.09}_{-0.12}$
CGRO/OSSE	50–150 keV	McNaron-Brown	19.29	24–27	$-29.63^{+0.26}_{-0.70}$ (4)	3–6	$-29.55^{+0.19}_{-0.35}$ (4)
ASCA	2–10 keV	Makino	17.86[b]	27.5	-29.05 ± 0.05 (1)	...	...
RXTE	1–10 keV	McHardy	17.68[b]	24.8–27.9	-28.91 ± 0.06 (4)	4.2–5.5	$-28.51^{+0.14}_{-0.21}$ (2)
ROSAT/HRI	0.1–2.4 keV	Madejski	17.08[b]	17	-28.53 ± 0.05 (1)	...	...
HST/FOS	1300–2240 Å	Stocke	15.35	8	-26.59 ± 0.01 (1)	...	...
IUE/SWP	1400–1600 Å	Ghisellini & Webb	15.30	25.4	-26.58 ± 0.04 (1)	...	...
IUE/LWP	2500–2700 Å	Ghisellini & Webb	15.06	24.6–27.4	-26.25 ± 0.05 (3)	5.4	-26.12 ± 0.02 (1)
Optical Photometry from Ground-based Telescopes	*B*	see Table 2	14.83	28	-25.85 ± 0.02 (1)	...	...
	V	see Table 2	14.74	25.4–28	-25.70 ± 0.02 (7)	...	...
	R	see Table 2	14.67	25.4–28	-25.57 ± 0.02 (8)	4.3	-25.40 ± 0.02 (1)
	I	see Table 2	14.58	25.4	-25.39 ± 0.03 (5)	...	...
CTIO (1.5m+NIC)	*J*	Backman	14.38	31	-25.00 ± 0.01 (1)	3	-24.903 ± 0.006 (1)
	H	Backman	14.26	31	-24.86 ± 0.041 (1)	3	-24.74 ± 0.01 (1)
	K	Backman	14.13	31	-24.61 ± 0.021 (1)	3	-24.556 ± 0.007 (1)
JCMT	0.45 mm	Stevens	11.82	...	...	5–6	$-22.04^{+0.09}_{-0.11}$ (2)
	0.8 mm	Stevens	11.57	...	...	5–6	-21.91 ± 0.04 (2)
	1.1 mm	Stevens	11.44	...	...	5–6	-21.83 ± 0.03 (2)
	1.3 mm	Stevens	11.36	...	...	5–6	-21.83 ± 0.06 (2)
	2 mm	Stevens	11.18	...	...	5–6	-21.75 ± 0.04 (2)
IRAM	250 GHz	Freudling	11.40	13	$-21.58^{+0.12}_{-0.16}$ (2)	...	...
Metsähovi Station	37 GHz	Teräsranta	10.57	26–27	-21.65 ± 0.02 (2)	7	-21.59 ± 0.01 (1)
	22 GHz	Teräsranta	10.34	26–27	-21.65 ± 0.01 (2)	4–6	-21.64 ± 0.01 (2)
UMRAO	14.5 GHz	M. Aller & H. Aller	10.16	22.5	-21.743 ± 0.006 (2)	...	...
	8 GHz	M. Aller & H. Aller	9.90	28.4	-21.838 ± 0.007 (1)	4.4	-21.829 ± 0.004 (1)
	4.8 GHz	M. Aller & H. Aller	9.68	25.4–26.4	-21.945 ± 0.005 (2)	...	...

[a] Fluxes in the low and flaring state were obtained by averaging the data in the intervals designated in the respective preceding columns. The number of averaged data points is reported in parentheses. Uncertainties represent standard deviations from the mean values. If only one observation is available, or if the dispersion is less than the typical intrinsic error, the latter is given.

[b] For *ASCA*, *RXTE*, and *ROSAT*/HRI, the frequencies listed correspond to 3, 2, and 0.5 keV, respectively.

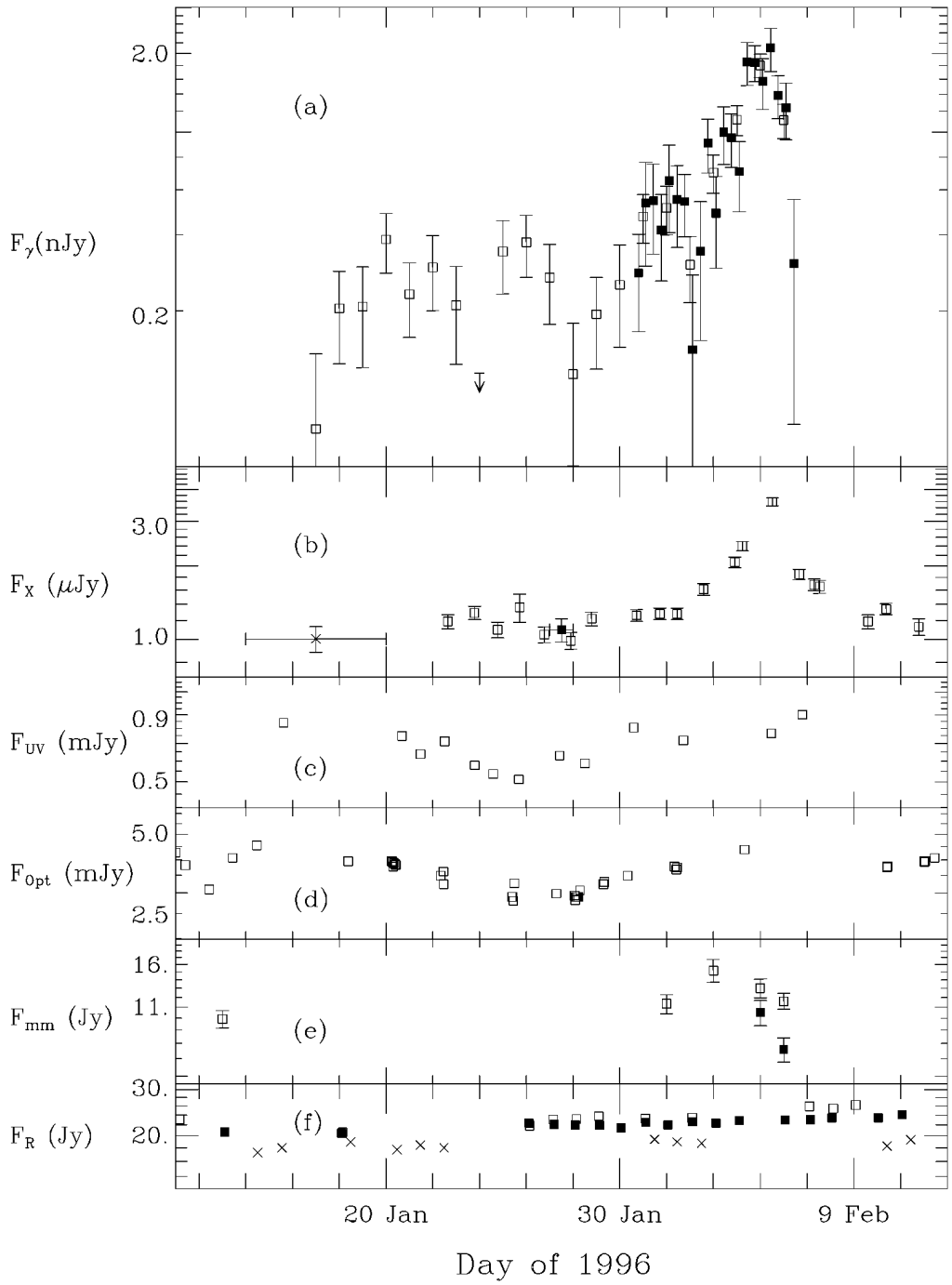

FIG. 1.—Multiwavelength light curves of 3C 279 during the EGRET campaign (1996 January 16–February 6): (*a*) EGRET fluxes at greater than 100 MeV binned within 1 day (*open squares*) and 8 hr (*filled squares*) (referred to 400 MeV as for Thompson et al. 1996); (*b*) X-ray fluxes at 2 keV: besides the *RXTE* data (*open squares*), the isolated *ASCA* (*filled square*) and *ROSAT*-HRI (*cross*) points are reported with horizontal bars indicating the total duration of the observation; (*c*) *IUE*-LWP fluxes at 2600 Å; (*d*) optical data from various ground-based telescopes in the *R* band; (*e*) JCMT photometry at 0.8 mm (*open squares*) and 0.45 mm (*filled squares*); (*f*) radio data from Metsähovi at 37 GHz (*open squares*) and 22 GHz (*filled squares*), and from UMRAO at 14.5 GHz (*crosses*). Errors, representing 1-σ uncertainties, have been reported only when they are bigger than the symbol size.

During the *CGRO* observations from 1996 January 16–30, 3C 279 was close to the center of the field of view of EGRET and COMPTEL (5°.0–6°.7). OSSE began observations on 1996 January 24. Due to the outstanding brightness detected by EGRET, the pointing was extended through 1996 February 6 as part of a Target of Opportunity program.

The high emission state of 3C 279 made it possible to detect a significant signal with EGRET for integration times of 1 day and even of 8 hr during the flare. The light curves are shown in Figure 1*a*. Analysis of the EGRET spectrum during the flare (from February 4–6) yielded an energy index $\alpha_\nu = 0.97 \pm 0.07$ between 30 MeV and 10 GeV, and $\alpha_\nu = 1.07 \pm 0.09$ was found for the period January 16–30. We use the convention $f_\nu \propto \nu^{-\alpha_\nu}$.

COMPTEL detected the source at energies above 3 MeV. Over the whole period, the average flux in the 10–30 MeV band was $(2.6 \pm 0.6) \times 10^{-5}$ photons s^{-1} cm^{-2}. The

average energy spectrum tends to be hard (power-law photon index less than 2); however, the power-law slope cannot be determined accurately as a result of nondetection below 3 MeV.

The source was in the OSSE field of view from January 24 to February 7 and was detected in each of the 2 weeks at a high confidence level.

The *RXTE* satellite began observing 3C 279 less than a month after launch and monitored the source for 20 minutes daily, from January 21 to February 10, during its performance verification phase (McHardy et al. 1998). This was preceded by 6 days of observations with the *ROSAT* HRI (January 14–20) and accompanied by one 20 ks *ASCA* pointing on January 27 (Makino et al. 1996). The *RXTE* data were calibrated by performing background subtraction from slewing data; the *ASCA* spectral index $\alpha_\nu = 0.7$ was used to calculate flux densities. The robustness of the *RXTE* background modeling is demonstrated by the agreement of the flux densities at the low end of the *RXTE* energy range and the high end of the *ROSAT* energy range on the day(s) in which their coverage overlapped. The X-ray light curve is shown in Figure 1*b*.

IUE observed 3C 279 at approximately daily intervals from January 15.6 to February 6.8 with the LWP camera and on one occasion (January 25) with the SWP. The 13 LWP spectra were reduced and calibrated according to the Final Archive processing routine that adopts the New Standard Image Processing System (NEWSIPS) method for spectral extraction (Nichols & Linsky 1996). Lyα emission (1216 Å) is clearly visible on the SWP spectrum redshifted to $\sim$1870 Å, with a dereddened intensity of $(5 \pm 2) \times 10^{-14}$ ergs s^{-1} cm^{-2}. No emission line is present in the LWP spectra. The LWP spectral signal was integrated and averaged in the 2500–2700 Å interval, where the camera sensitivity is highest and the solar scattered-light contamination (which might have been present in the first half of the monitoring) is negligible. The SWP signal was averaged in the 1400–1600 Å range, where the camera sensitivity is high and no emission lines are superposed on the continuum. Uncertainties are computed as in Falomo et al. (1993). The LWP light curve is shown in Figure 1*c*.

The source was observed just before the start of the multifrequency campaign on 1996 January 8 with the *HST* Faint Object Spectrograph, using the G130H and G190H gratings exposed for 2820 and 2250 s, respectively, as part of a different program whose results will be reported elsewhere (Stocke et al. 1998). The shape of the dereddened spectral flux distribution in the interval 1300–2240 Å is described by a power-law with energy index $\alpha_\nu = 1.81 \pm 0.05$. Although not obtained during the EGRET pointing, these data are of interest here since they yield a reliable measure of the Lyα intensity, which is important in estimating the inverse Compton contribution from external seed photons. The dereddened line intensity is $(4 \pm 1) \times 10^{-14}$ ergs s^{-1} cm^{-2}.

Optical *BVRI* photometry was obtained at several different sites listed in Table 2. The *R* band has the best temporal coverage, including one point close to the peak of the γ-ray flare, so only those data are shown in Figure 1*d*. The data in the *B* band are very sparse; those in the *V* and *I* bands show the same behavior as the *R*-band light curve within the uncertainties. The conversion of optical magnitudes to fluxes has been done following Bessel (1979). For a presentation of the complete data set of ground-based optical, near-IR, millimeter, and radio observations, as well as for the *IUE* data related to this campaign, we defer to a separate paper.

The near-IR emission of 3C 279 was measured in the *J*, *H*, and *K* bands at Cerro Tololo Inter-American Observatory (CTIO) on January 31 and February 3. Only two data points were obtained within the timespan of the campaign for each filter (Table 1). The conversion from *JHK* magnitudes to fluxes follows Bersanelli, Bouchet, & Falomo (1991).

The source was observed at millimeter and submillimeter wavelengths at the James Clerk Maxwell Telescope with both heterodyne and bolometer receivers as part of an extensive campaign that lasted through 1996 June. Few observations were obtained during the campaign reported here, but they were close in time to the γ-ray peak. The 0.45 and 0.8 mm data are shown in Figure 1*e*. At longer wavelengths the variations were smaller.

Bolometric observations at millimeter wavelengths were carried out with the 30 m IRAM telescope using the IRAM/MPI seven-channel bolometer on 1996 January 13. The nominal frequency of the bolometer is 250 GHz, and the bandwidth is about 60 GHz. The observations were carried out under poor weather conditions. Observations of Uranus in the same night after weather conditions significantly improved were used for the flux calibration, assuming a flux of 35.18 Jy. The standard, recommended gain-elevation correction was applied. The resulting fluxes of the two observations were 33.7 ± 0.3 Jy and 18.2 ± 1.1 Jy, where the errors are the rms of the single scans within each observation. We attribute the difference in the results

TABLE 2

OPTICAL PHOTOMETRIC MONITORING OF 3C 279 IN 1996: OBSERVERS AND INSTRUMENTS

Observer	Observatory	Telescope	Filters	Dates
Aldering	CTIO	0.9 m	BRI	Jan 27–29
Backman	NURO, Lowell	0.8 m	BVRI	Jan 12
Balonek	Foggy Bottom	16″	VR	18 Jan–Apr 22
Balonek	Case Western Reserve Univ.	Burrell Schmidt	R	Jan 8–14
Boltwood	Boltwood	18 cm	VRI	20 Jan–10 Mar
Falomo	ESO	NTT	V	18.1 Jan
Ghisellini & Villata	Torino	REOSC 1.05 m	BVR	4 Jan–7 Apr
Hall	Steward	90″	griz (Gunn)	28, 30 Jan
Kidger & Gonzalez-Perez	Tenerife	82 cm	BVR	7, 10 Jan
Nair	University of Florida	30″	VR	19 Feb
Takalo & Sillanpää	Tuorla	1.03 m	BVR	26 Jan–12 Feb
Smith	Steward	90″	V	27 Jan
Tosti	Perugia	0.4 m	VRI	23 Feb–20 May

to the changing weather conditions and adopt a value of 26 ± 8 Jy.

Radio observations at 37 and 22 GHz were conducted at the Metsähovi Radio Research Station from January 3 to February 11 and at 4.8, 8, and 14.5 GHz from January 2 to March 1 at the University of Michigan Radio Astronomical Observatory as part of long-term monitoring programs. The resulting light curves at the three highest radio frequencies are shown in Figure 1*f*.

3. COMPARISON OF MULTIWAVELENGTH LIGHT CURVES

The 1 day binned EGRET light curve shows an extraordinary flare peaking on February 5 (Fig. 1*a*). Before January 30, the fluctuations visible to the eye in the γ-ray light curve are probably not due to real variability (the probability of variability is 30%, according to a χ^2 test). The peak flux represents an increase by a factor of 10 with respect to the average level between January 20 and 30. The 8 hr binned EGRET light curve during the outburst appears modulated by high-amplitude variations, the largest of which, a factor of 4–5 in 1 day, has a doubling time of only $\tau_D = 6$ hr $[\tau_D \equiv (F_{\rm initial}/\Delta F)\Delta t]$.

Between the January 16–30 and the Target-of-Opportunity periods, the flux in the 10–30 MeV range (COMPTEL) increased by a factor of 3.6 (2.5 σ significance level).

No significant variability on timescales of days was found in the OSSE data, according to a χ^2 test.

The X-ray light curve also shows a large outburst, well correlated in time with the γ-ray flare but of lower amplitude (factor of 3, Fig. 1*b*). Any possible lag is less than the temporal resolution of 1 day, as confirmed by an analysis with the discrete correlation function method (DCF, Edelson & Krolik 1988). The width of the outburst is about 7 days in X-rays, where the data extend from the preflare state to the decay, while the γ-ray coverage ends 1 day after the flare peak. The *ROSAT* HRI data did not reveal any variability larger than 10%; therefore, the average 1 keV flux has been reported here as well as for the *ASCA* observation.

The light curve at 2600 Å (*IUE* LWP) is reasonably well sampled during the first part of the campaign but not toward the end, when the γ-ray flare occurred (Fig. 1*c*). It shows a broad minimum at $\sim$January 25–26, followed by a rise of almost a factor of 2, but with a 3 day gap before and up to the γ-ray peak. If the UV minimum were associated with the (possible) minimum in the EGRET light curve at January 28, this would indicate a correlation, with the UV leading the γ-rays by $\sim$2.5 days. In this case the UV maximum would have occurred before the γ-ray peak, during the gap in *IUE* monitoring between February 1 and 5. Unfortunately, the UV and γ-ray light curves have too few points to apply the DCF method efficiently, so no robust result can be found from their cross-correlation.

The *R*-band light curve is similar to the UV light curve in showing a broad minimum on days January 26–28, followed by a rise (Fig. 1*d*). Again, the sampling around the γ-ray flare is very poor. One observation very close to the flare peak yields a flux higher than the average around day January 28 by a factor of 1.6. The behavior in *V* and *I* (not shown) is similar. On the whole, the optical light curves suggest that their minimum occurs later than the UV minimum by 1–2 days. They resemble the γ- and X-ray light curves in the flare rise but differ significantly in having values quite close to those at the peak and also at other epochs (e.g., around January 20), when the high-energy light curves have values much lower than the peak. In other words, the flare stands out in the high-energy light curves, while it is not apparent as such in the UV-optical light curves.

A near-infrared flux increase was observed, whose amplitude is a factor of 1.3 in *J* and *H* band and 1.2 in *K* band. Therefore, within the limited sampling, the *JHK* data are consistent with the rising trend of the other light curves.

The submillimeter data are rather sparse but show variability consistent with the occurrence of a flare around February 3 (Fig. 1*e*). The sparse sampling prevents us from determining conclusively that the submillimeter peak actually occurred on February 3; it could as well have occurred on January 30, 31 or February 1, 2. Observations at 0.45, 0.8, 1.1, 1.3, and 2 mm on February 5 and 6 show a decline in flux, of decreasing amplitude with increasing wavelength, corresponding to the γ- and X-ray decline after the outburst. We notice that the level of the millimeter/submillimeter flux reached during the present campaign has been exceeded only once (in 1994) in the last 7 yr, and in 1996 May a further increase by 20%–30% was recorded.

At radio frequencies the variability is highly significant (Fig. 1*f*). There is a nearly monotonic increase of $\lesssim$30% amplitude at 37 GHz from January 18 to February 9 and a smaller increase at lower frequencies. A 6–7 Jy rise in 20 days is rare in the 16 yr Metsähovi database. The brightness reached its historic maximum (since 1980) during 1996 May–June, a time delay of about 4 months relative to the X-and γ-ray flare.

4. RADIO–TO–γ-RAY ENERGY DISTRIBUTIONS

The multiwavelength data collected during the 1996 monitoring campaign allow us to follow the evolution of the overall spectrum of 3C 279 from a quasi-stationary state through the development of a dramatic, high-energy outburst. There is no unique definition of a preflare state. In Figures 2 and 3 we show average fluxes in the period January 24–28 (where available), which includes the UV and optical minima.

The epoch of the high-energy outburst is well covered at most wavelengths, no more than 2 days from the γ-ray peak. We can therefore construct a reliable spectral energy distribution (SED) for the highest state. We averaged the available data in a 2-day window centered on the γ-ray peak (February 4–6). The resulting SED for the flaring state is shown in Figures 2 and 3.

Near-IR, optical, and UV data (Table 1) have been corrected (shown in Figs. 2 and 3) according to Cardelli, Clayton, and Mathis (1989) for Galactic interstellar extinction, using $N_{\rm H} = 2.22 \times 10^{20}$ cm^{-2} (Elvis et al. 1989), a gas-to-dust ratio $N_{\rm H}/E_{B-V} = 5.2 \times 10^{21}$ cm^{-2} mag^{-1} (Shull & Van Steenberg 1985), and a total-to-selective extinction ratio $A_V/E_{B-V} = 3.1$ (Rieke & Lebofsky 1985). The X-ray count rates have been converted to flux units, using a power-law energy index of 0.7 derived from the *ASCA* 2-10 keV observations. The γ-ray photon counts have been converted to fluxes at 0.4 GeV according to Thompson et al. (1996).

The spectrum consists of two broad humps with peaks at $\sim 10^{12} - 10^{13}$ Hz and $10^{22} - 10^{24}$ Hz. *ISO* data (Barr et al. 1998) will be of great importance to determine the shape of the SED in the range where the maximum synchrotron

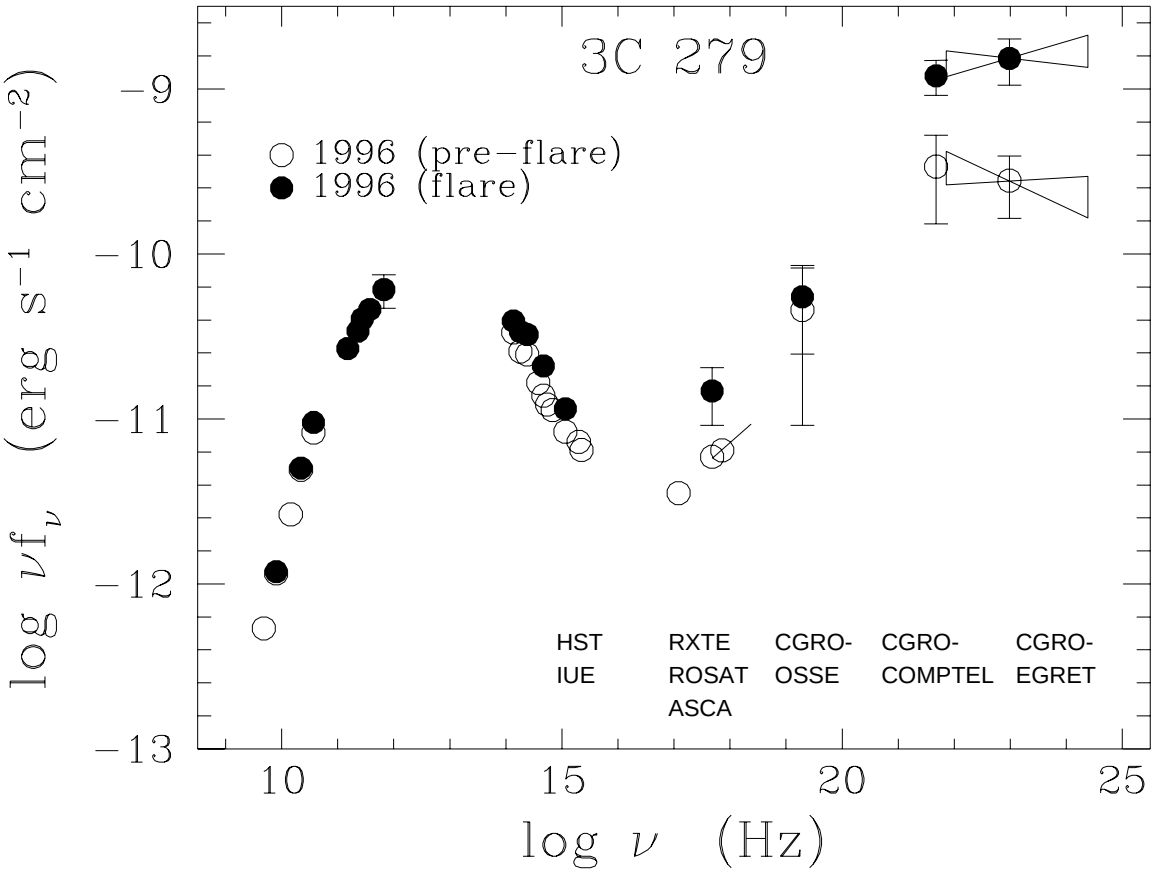

FIG. 2.—Radio–to–γ-ray energy distribution of 3C 279 in low (*open circles*) and flaring state (*filled circles*) in 1996 January–February. The data plotted correspond to the entries of Table 1, except that the UV, optical, and near-IR data have been corrected for Galactic extinction (see text). The slope of the *ASCA* spectrum ($\alpha_\nu = 0.7$) has been reported normalized to the *RXTE* point closest in time. The EGRET best-fit power-law spectra referring to the January 16–30 (low state) and February 4–6 periods are shown, normalized at 0.4 GeV. Errors have been reported only when they are bigger than the symbol size.

power is expected to be emitted. It is interesting to note that the submillimeter spectral slope during the flare ($\alpha_\nu = 0.38 \pm 0.09$ on February 5 and $\alpha_\nu = 0.51 \pm 0.08$ on February 6) is roughly the same as the hard X-ray to MeV–γ-ray spectrum ($\alpha_\nu \sim 0.6$), as expected if the same electrons are responsible for the synchrotron and inverse Compton-scattered radiation at those energies.

Comparing the flare and preflare states, it is clear that the high-energy spectrum (X- to γ-rays) is harder at the flare peak, as implied by the larger amplitude of the γ-ray variation.

From near-IR to UV frequencies, the flare versus preflare variations are smaller than in X- and γ-rays. Comparing simultaneous J, H, and K fluxes at two epochs suggests again that the variability amplitude increases with frequency, but the effect does not show up when comparing UV to V-, R-, or I-band variations. There is little information on the preflare fluxes at still lower frequencies except for the radio band, which is only weakly coupled to the rest of the SED. We note, however, that from the few data points available, the amplitude of the variations at 0.45 and 0.8 mm is comparable to that of the simultaneous X-ray variations.

The SEDs of 3C 279 obtained during the 1991 June high state and the 1993 January low state are also shown in Figure 3 for comparison with the flare and preflare SEDs derived here. The 1991 γ-ray data are averaged over the 2 week pointing which included the flare. The X-ray and R-band observations were simultaneous. The other measurements were close in time, except for the UV spectrum, which was obtained one month later (Hartman et al. 1996).

5. DISCUSSION

In early 1996, the blazar 3C 279 was observed in its highest γ-ray emission state ever. The preflare flux level (before 1996 February 1) was comparable to the average state in 1991 June (Kniffen et al. 1993; Hartman et al. 1996). The presently observed maximum exceeds by a factor of ~ 3 the peak of the 1991 June 24–25 outburst, the brightest state recorded previously, and is ~ 90 times higher than the historical γ-ray minimum seen with EGRET in 1992 December–1993 January (Maraschi et al. 1994).

Inspection of Figure 1 indicates decreasing variability amplitude with decreasing energy (within either the synchrotron or inverse Compton component), which is a common characteristic of blazar variability (e.g., 3C 279 itself, Maraschi et al. 1994; PKS 2155–304, Urry et al. 1997). In addition, the X-ray emission during the 1996 outburst was higher than measured in 1991 June with *Ginga* over approximately the same energy range (Fig. 2). Thus, not only is the X-ray variability amplitude lower than the γ-ray during the 1996 flare, but over longer timescales the overall amplitude is also lower. Notice that the flaring multiwavelength SED in 1996 February presents an "inverted" variation with respect to the 1991 state: the γ-ray flux is *higher* than in 1991 by a factor of ~ 4, and the optical-UV

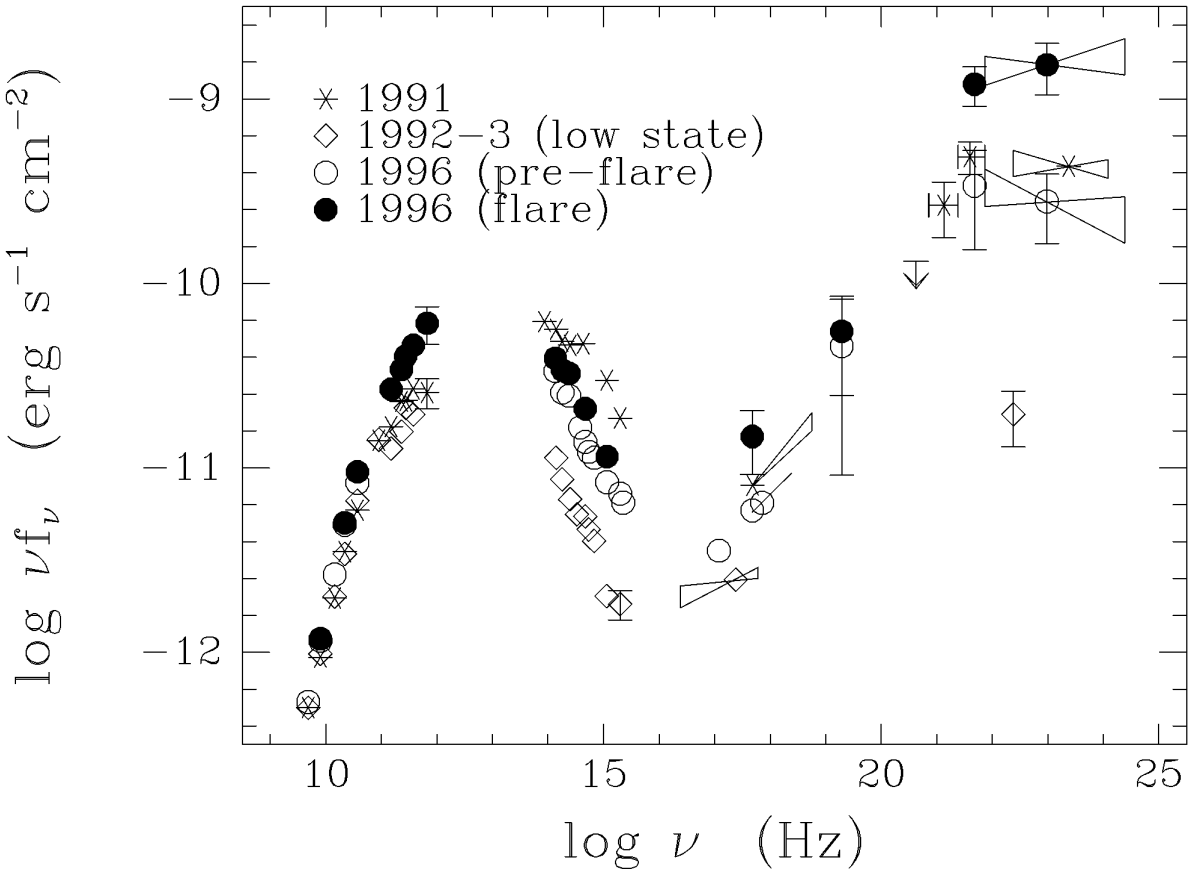

FIG. 3.—Radio–to–γ-ray energy distribution of 3C 279 in low (*open circles*) and flaring state (*filled circles*) in 1996 January–February. The data plotted correspond to the entries of Table 1, except that the UV, optical, and near-IR data have been corrected for Galactic extinction (see text). The slope of the *ASCA* spectrum ($\alpha_\nu = 0.7$) has been reported normalized to the *RXTE* point closest in time. The EGRET best-fit power-law spectra referring to the January 16–30 (low state) and February 4–6 periods are shown, normalized at 0.4 GeV. For comparison, the SEDs in 1991 June (*stars*) and in 1992 December–1993 January (*diamonds*) are also shown (see Maraschi et al. 1994). Errors have been reported only when they are bigger than the symbol size.

flux is *lower* than earlier by a factor of $\sim$1.5–2.

During the 1996 observations, significant γ-ray variability was found on timescales comparable to the sampling resolution (i.e., 8 hr). Such extremely fast variability has also been found in several other blazars (Hartman 1996; Mattox et al. 1997). The amplitude and rapidity of these luminosity changes exceed a well-known limit based on accretion efficiency (Fabian 1979; Dermer & Gehrels 1995), which probably occurs in blazars because their observed radiation comes from relativistically beamed jets (with unknown relation to accretion processes).

The simultaneous variability in X-rays and GeV γ-rays shows for the first time that they are approximately cospatial. This, plus the rapid γ-ray variability, gives a strong lower limit to the beaming factor from the condition that the emission region should be transparent to γ-rays ($\tau_{\gamma\gamma} \propto \delta^{-5} L/\Delta t$). For the optical depth to photon-photon absorption to be less than unity, the required beaming factor is $\delta_\gamma \geq 6.3$ or $\delta_\gamma \geq 8.5$ for photons of $\sim$1 or $\sim$10 GeV, respectively. These values are derived following Dondi & Ghisellini (1995) but are somewhat larger than theirs because of the faster variability now observed. An independent argument for relativistic bulk motion of the low-frequency emitting region comes from the limit to the X-ray flux produced by the self-Compton process (Marscher et al. 1979), which gives $\delta \geq 18$ (Ghisellini et al. 1993). A third estimate comes from the observed superluminal expansion of VLBI-resolved knots, $\delta \sim 6$ (preliminary estimate from Wehrle et al. 1998).

In low-frequency peaked blazars like 3C 279, high-energy electrons in a relativistic jet radiate at radio-through-UV wavelengths via the synchrotron process, and can produce X- and γ-rays by scattering soft-target photons present either in the jet (SSC) or in the surrounding "ambient" (EC—Maraschi, Ghisellini, & Celotti 1992; Blandford 1993; Dermer, Schlickeiser, & Mastichiadis 1992; Sikora, Begelman, & Rees 1994). The relative variability in the synchrotron and inverse Compton components can indicate the origin of these seed photons. Specific, time-dependent models are clearly necessary for an in-depth discussion but are beyond the scope of this paper. In the following we discuss in general terms different scenarios for the origin of the seed photons, assuming that a single, active "blob" in the jet is responsible for the variability.

The SSC model predicts that a change in the electron spectrum (intensity and/or shape) should cause larger variability in the inverse Compton emission than in the synchrotron emission because the energy densities of the seed photons and the scattering electrons vary in phase. In a one-zone model, the peak flux of the inverse Compton SED should vary approximately quadratically with the peak flux of the synchrotron distribution (Ghisellini & Maraschi 1996).

Between 1991 June and 1993 January this quadratic

variation condition was satisfied, assuming the synchrotron peak was close to the IR band (Maraschi et al. 1994; Ghisellini & Maraschi 1996), but for the 1996 flare versus preflare SEDs the amplitude of the γ-ray variation is *more than the square* of the IR-optical-UV flux variation. However, there are very few data close to the γ-ray maximum (the IR points are from February 3, which is at half-maximum), and the synchrotron peak may also fall at lower frequencies ($\sim 10^{13}$ Hz, as suggested by the strong flux at millimetric wavelengths), where adequate variations could have occurred. A further caveat is that different emission zones could contribute to the IR-optical flux, diluting the intrinsic variation due to the γ-ray–emitting region. We conclude that the SSC scenario can not be ruled out by the present data.

Alternatively, we consider the EC scenario (Sikora, Begelman, and Rees 1994), where the seed photons are external to the jet and independent of it. In this case, (1) the inverse Compton emission should vary linearly with the synchrotron emission for changes in the electron spectrum, and (2) larger than linear variations of the inverse Compton emission can be explained if the bulk Lorentz factor of the emission region varies together with the electron spectrum. In the latter case, the different beaming patterns of synchrotron and inverse Compton radiation should also be taken into account (Dermer 1995). As also happens for the SSC model, different emission zones contributing to the IR–optical flux would dilute the intrinsic variation because of the γ-ray–emitting region.

While the second case is conceivable comparing SEDs separated by years, it is far less likely that the entire emission region could accelerate *and decelerate* significantly over the timescale of the rapid flare observed here. The first case is unlikely because of the apparent nonlinear response of the γ-rays to the synchrotron variability.

An interesting alternative that combines advantages of both the SSC and EC scenarios is the "mirror" model of Ghisellini & Madau (1996). Here the seed photons are provided by rapidly varying, broad line emission from a few clouds close to the jet and photoionized by an active blob in it. First, the photoionizing continuum is beamed and therefore intense and highly variable; second, the electrons in the jet see broad line emission from the nearest cloud(s) as beamed; and, third, the γ-ray–emitting blob, approaching the clouds, will see an increasing radiation energy density due to the decreasing blob-cloud distance. These effects lead to a more than quadratic increase in γ-rays, associated with variations in synchrotron emission from the active blob. This picture requires rather special conditions, in that the cloud(s) close to the jet must also have a large covering factor to let their emission-line flux dominate the radiation energy density seen by the blob.

The observations presented here can be accounted for by the mirror model if the far-UV (photoionizing) emission varied during the flare by a factor of 3–4. This was not directly observed but is consistent with an extrapolation from the UV variations. If an increase occurred as an active region of the jet approached one or more broad emission line clouds lying within the jet's beam, then the observed amplitude of γ-ray variability could be explained, at least qualitatively. Also, the asymmetric shape of the X-ray curve—in which the decay is possibly faster than the rise—can be accommodated by the mirror model, since the inverse Compton emission drops sharply (because of the narrow angular pattern of the beaming) once the active part of the jet passes the broad emission line cloud(s).

We note that no variations in the Lyα luminosity are seen in archival (*IUE* and *HST*) spectra of 3C 279—as opposed to a large historical variability of the continuum—implying that a steady component, like an accretion disk rather than the jet beam, dominates the overall photoionization of the broad emission line clouds (Koratkar et al. 1997). However, the jet could still play a significant role in powering the clouds close to it. The mirror model could be tested in principle, even in the absence of any available γ-ray observations, by monitoring the Lyα emission line of 3C 279. A limited number of clouds over a limited velocity range should respond simultaneously to the most rapidly varying (timescales of days) jet emission. However, the observed variability amplitude may be small, being diluted by the overall broad emission line region emission.

The line-intensity measurements of January 8 and 25 from the *HST*-FOS and *IUE*-SWP spectra, respectively, that indicate no change are inconclusive because they both refer to the preflare epoch and to similar continuum levels. Moreover, the *IUE* sensitivity is far too low to measure variations in the line profile.

6. SUMMARY

Radio–to–γ-ray monitoring of the blazar 3C 279 in 1996 January–February recorded the highest γ-ray flux of the source ever measured. A correlated flare at X- and γ-ray energies with an amplitude of a factor 3 and 10, respectively, is seen and completely resolved. The data at optical and UV frequencies clearly show a flux increase correlated with the X- and γ-ray rise, although the poor sampling close to the flare peak prevents a precise measurement of the amplitude in these bands. The millimetric flux—measured only close to the flare peak—shows variability that could be correlated with the high energy light curves. The radio emission exhibited variations of remarkable rapidity and amplitude.

The relative amplitudes of the high-energy and low-energy light curves during the flare, and the apparently stronger IR to UV emission in 1991 June (when the average γ-ray flux was weaker), represent important challenges for our understanding of blazars.

The data do not rule out SSC models—especially if more than one zone contributes to the emission—but are difficult to reconcile with a scenario in which the seed photons are provided by the ambient medium surrounding the jet and independent from it. A picture in which the relativistic jet hits and ionizes a small fraction of the broad emission line clouds, which then provide the photons to be inverse-Compton upscattered, seems appealing and likely. Sensitive measurements of variations in the profile of the strong Lyα line, correlated with the beamed UV continuum, could test this model.

We are grateful to the staffs of *ISO*, *IUE*, *HST*, *ASCA*, *ROSAT*, *XTE*, *CGRO*, CTIO, JCMT, IRAM, IAC Tenerife, Metsähovi Station, UMRAO, NURO, Lowell Observatory, Boltwood Observatory, Foggy Bottom Observatory, the Burrell Schmidt Observatory of Case Western Reserve University, the ESO NTT, the observatories of Torino, Tuorla, Perugia and the University of Florida. We thank Charles Dermer for his comments on the

paper. A. E. W., S. C. U., and W. X. acknowledge support from the NASA Long Term Space Astrophysics Program. E. P. is grateful for hospitality at IPAC during development of this research and acknowledges support from NASA Long Term Space Astrophysics Program. C. M. U., E. P., and J. E. P. acknowledge support from NASA grants NAG 8-1037, NAG 5-2538, and NAG 5-3138. J. R. W. acknowledges support from NASA *IUE* Guest Observer Program. M. F. A. and H. D. A. acknowledge support from NSF grant AST 94-21979. D. E. B., J. D. and G. S. A. were Visiting Astronomers at CTIO, National Optical Astronomy Observatories, operated by the Association of Universities for Research in Astronomy, Inc. (AURA), under a cooperative agreement with the NSF. The National Undergraduate Research Observatory (NURO) is operated by Lowell Observatory under an agreement with Northern Arizona University and the NURO Consortium. The observers from Franklin and Marshall College thank the University of Delaware/Bartol Research Institute's Space Grant Colleges consortium for partial support of NURO membership and observations. The James Clerk Maxwell Telescope is operated by The Joint Astronomy Centre on behalf of the Particle Physics and Astronomy Research Council of the United Kingdom, the Netherlands Organization for Scientific Research, and the National Research Council of Canada. We thank C. Imhoff, N. Loiseau, and J. Nichols for assistance with *IUE* observations and data reduction, and E. Solano and W. Wamsteker for timely NEWSIPS reprocessing of part of the *IUE* spectra. Portions of the research described in this paper were carried out by the Jet Propulsion Laboratory, California Institute of Technology, under a contract with NASA.

REFERENCES

Barr, P., et al. 1998, in preparation
Bersanelli, M., Bouchet, P., & Falomo, R. 1991, A&A, 252, 854
Bessel, M. S. 1979, PASP, 91, 589
Blandford, R. D. 1993, in AIP Conf. Proc. 280, Compton Gamma-Ray Observatory, ed. M. Friedlander, N. Gehrels, & D. J. Macomb (New York: AIP), 533
Cardelli, J. A., Clayton, G. C., & Mathis, J. S. 1989, ApJ, 345, 245
Dermer, C. D. 1995, ApJ, 446, L63
Dermer, C. D., & Gehrels, N. 1995, ApJ, 447, 103
Dermer, C. D., Schlickeiser, R., & Mastichiadis, A. 1992, A&A, 256, L27
Dondi, L., & Ghisellini, G. 1995, MNRAS, 273, 583
Edelson, R. A., & Krolik, J. H. 1988, ApJ, 333, 646
Elvis, M., Lockman, F. J., & Wilkes, B. J. 1989, AJ, 97, 777
Fabian, A. C. 1979, Proc. R. Soc. London A, 366, 449
Falomo, R., Treves, A., Chiappetti, L., Maraschi, L., Pian, E., & Tanzi, E. G. 1993, ApJ, 402, 532
Ghisellini, G., & Madau, P. 1996, MNRAS, 280, 67
Ghisellini, G., & Maraschi, L. 1996, in ASP. Conf. Proc. 110, Blazar Continuum Variability, ed. H. R. Miller, J. R. Webb, & J. C. Noble (San Francisco: ASP), 436
Ghisellini, G., Padovani, P., Celotti, A., & Maraschi, L. 1993, ApJ, 407, 65
Hartman, R. C. 1996, in ASP. Conf. Proc. 110, Blazar Continuum Variability, ed. H. R. Miller, J. R. Webb, & J. C. Noble (San Francisco: ASP), 333
Hartman, R. C., et al. 1996, ApJ, 461, 698
———. 1998, in preparation
Kniffen, D. A., et al. 1993, ApJ, 411, 133
Koratkar, A. P., Pian, E., Urry, C. M., & Pesce, J. E. 1998, ApJ, 492, 173
Makino, F., Inoue, H., Kii, T., Nagase, F., & Yamashita, A. 1996, IAU Circ. 6302
Maraschi, L., Ghisellini, G., & Celotti, A. 1992, ApJ, 397, L5
Maraschi, L., et al. 1994, ApJ, 435, L91
Marscher, A. P., Marshall, F. E., Mushotzky, R. F., Dent, W. A., Balonek, T. J., & Hartman, M. F. 1979, ApJ, 233, 498
Mattox, J. R., Wagner, S. J., Malkan, M., McGlynn, T. A., Schachter, J. F., Grove, J. E., Johnson, W. N., & Kurfess, J. D. 1997, ApJ, 476, 692
McHardy, I. M., et al. 1998, in preparation
Nichols, J. S., & Linsky, J. L. 1996, AJ, 111, 517
Pian, E., et al. 1998, in preparation
Rieke, G. H., & Lebofsky, M. J. 1985, ApJ, 288, 618
Shull, J. M., & Van Steenberg, M. E. 1985, ApJ, 294, 599
Sikora, M., Begelman, M. C., & Rees, M. J. 1994, ApJ, 421, 153
Stocke, J., et al. 1998, in preparation
Thompson, D. J., et al. 1995, ApJS, 101, 259
———. 1996, ApJS, 107, 227
Ulrich, M.-H., Maraschi, L., & Urry, C. M. 1997, ARA&A, 35, 445
Urry, C. M., et al. 1997, ApJ, submitted
Webb, J. R., et al. 1996, in Tuorla Obs. Rep. N. 176, Workshop on Two Years of Intensive Monitoring of OJ 287 and 3C 66A, ed. L. O. Takalo (Turku: Tuorla Observatory), 20
Wehrle, A. E., et al. 1998, in preparation